Solar Energy
And Sustainable Development
Refereed, biannual scientific journal issued by:
The Libyan Center for Solar Energy Research and Studies

Geothermal Energy Utilization of Co-Production Water from Oilfields for Electric Power Generation

Ibrahim M. Abou El Leil[1]*, Seham N. Tawfic[2], Ahmed Mohammed[3].

[1]Petroleum Engineering Department, Faculty of Engineering, Tobruk University.
[2]Chemical Engineering Department, Faculty of Engineering, Tobruk University.
[3]Geology Department, Faculty of Science, Tobruk University.

E-*mail:* [1] ibrahim.aboueleil@tu.edu.ly ,[2] seham67@hotmail.com ,[3] ahmed.mohammed@tu.edu.ly .

SPECIAL ISSUE ON:

The 1st International Conference on Technical Sciences, 2024.
"Investing in Renewable Energies"
11 November 2024 SEBHA, LIBYA.

KEYWORDS

Geothermal energy, oilfields, co-production, temperature, power generation, power plant.

ABSTRACT

One significant source of geothermal energy is the co-produced hot water from oil/gas field production. There is potential to utilize oilfield infrastructure to produce geothermal electricity profitably, in a process called co-production. Due to the increasing demands of energy now days, this paper presents an investigation of geothermal energy production and utilization for electricity generation on the petroleum fields via organic Rankine cycle (ORC) technology, which is a reliable way to convert heat into electricity.

The current research focuses on the use of an ORC unit to generate electricity from co-produced water from ten oil wells in two oilfields, Jalo and Sarir. These wells refer to GX1, GX2, Gx3, GX4, GX5, SX1, SX2, SX3, SX4, and SX5, and they are combined in gathering centers (GC1) and (SC2) to utilize an existing medium-temperature geothermal source. The estimated total flow rates of co-produced water from the two gathering centers after separation are 5,728.34 BWPD and 14,618.65 BWPD respectively. Whereas, the geofluid mass flow rates from both oilfields are 12.25 kg/s and 34.05 kg/s, respectively, with an inlet geofluid (brine) temperature (T1) of 60°C and an outlet geofluid temperature (T2) of 35°C. The thermal efficiency (ηth) values for the Jalo and Sarir oilfields are 3.28% and 4.22%, respectively. According to the power output analysis, which indicates that the specific power outputs are 5.17 kW/kg/s and 9.85 kW/kg/s, and the gross power outputs are 63.33 kW and 338.80 kW, respectively, with a required hot water flow rate of 12.25 kg/s and 34.05 kg/s. This study revealed that the temperature and water flow rate are crucial factors affecting power output. By using an ORC plant, the generated electric power can be used in the field, supplied to the local grid, or utilized to offset on-field electricity consumption. Also, this study recommended by focusing efforts to extract the energy through electric power generation via production oil wells in oilfields.

*Corresponding author.

DOI: https://doi.org/10.51646/jsesd.v14iFICTS-2024.445

إستخدام الطاقة الحرارية الأرضية من المياه في الانتاج المشترك من حقول النفط لتوليد الطاقة الكهربائية

إبراهيم ابوالليل، سهام توفيق، أحمد محمد.

ملخص: تُعد المياه المُنتجة مع النفط/الغاز في الحقول النفطية أحد مصاد الطاقة الحرارية الأرضية المعتبرة. ومن الممكن استخدام البنية التحتية لحقول النفط لإنتاج الطاقة الكهربائية من الحرارة الأرضية على نحو مفيد وذلك من خلال عملية يُطلق عليها الإنتاج المشترك. ونظراً لتزايد الطلب على الطاقة في الوقت الراهن فإن هذه الورقة العلميّة تقدم دراسة حول إنتاج الطاقة الحرارية الأرضية واستخدامها في توليد الطاقة الكهربائية في حقول النفط من خلال تطبيق تقنيات دورة رانكين العضوية (ORC). هذه طريقة يمكن الاعتماد عليها لتحويل الحرارة إلى كهرباء، خاصة عندما تتوفر الحرارة الحرة في شكل طاقة متجددة مثل الطاقة الحرارية الأرضية. حيث تركز الدراسة الحالية على استخدام وحدة ORC لإنتاج الكهرباء من المياه المنتجة بشكل مشترك من عشرة آبار نفط في حقلين نفطيين هما جالو والسرير، واللذان يُشار إليهما بالرموز التالية GX1 و GX2 و Gx3 و GX4 و GX5 و SX1 و SX2 و SX3 و SX4 ، SX5 على التوالي، حيث يتم دمجهما في مركزي التجميع (GC1) و (SC2)، باستخدام مصدر الحرارة الجوفية المتوسطة الموجودة. وتبلغ تقديرات إجمالي معدل تدفق المياه المنتجة بشكل مشترك من الآبار الخمسة بعد عملية الفصل 5,728.34 برميل ماء/يوم و 14,618.65 برميل ماء/يوم بالنسبة للحقلين على التوالي، كما يبلغ معدل تدفق كتلة الماء 12.25 كجم/ثانية و 34.05 كجم/ثانية على التوالي، عند درجة حرارة الماء المُنتج (الماء الأجاج) عند المدخل (T1) البالغة 60 درجة مئوية ودرجة حرارة الماء عند المخرج (T2) البالغة 35 درجة مئوية. كما تبلغ الكفاءة الحرارية (ηth) لحقلي النفط جالو والسرير 3.28% و 4.22% على التوالي، وبناءً على تحليل إنتاج الطاقة، فقد تبين أن معدل إنتاج الطاقة هو 5.17 كيلووات/كجم/ثانية، 9.85 كيلووات/كجم/ ثانية، ويبلغ إجمالي إنتاج الطاقة 63.33 كيلوواط، 338.80 كيلوواط مع معدل تدفق الماء الساخن المطلوب 12.25 كجم/ثانية، 34.05 كجم/ثانية، كدالة لإنتاج الطاقة على التوالي، وقد أسفرت هذه الدراسة أن درجة الحرارة ومعدل تدفق الماء هما العاملان الأساسين لكمية الطاقة المتولدة في في محطة ORC، كما يمكن إنتاج الطاقة الكهربائية المحسوبة في الحقل وإمكانية توفيرها للشبكة المحلية أو استخدامها لموازنة استخدام الكهرباء في الحقل.

الكلمات المفتاحية – طاقة الحرارة الأرضية، حقول النفط، الإنتاج المشترك، درجة الحرارة، توليد القوى، محطة توليد الطاقة.

1. INTRODUCTION

Efficient reservoir management for oil and gas reservoirs involves addressing the disposal of co-produced water. The amount of water that needs to be disposed of varies depending on the specific reservoir and well. However, owing to water invasion, the volume of co-produced water increases as oilfields age. As the oil reservoir of Libya's Jalo oilfield has depleted over a period of 60 years, the current oil output has decreased to 120,000 barrels of oil per day (BOPD), whereas water production has increased to nearly 450,000 barrels of water per day (BWPD). Globally, the anticipated output of co-produced water is approximately 250 million barrels per day, whereas approximately 80 million barrels of oil are produced per day. This results in a water to oil ratio of approximately 3:1 or a 70% water cut. Over the past decade, the global water deficit has been increasing. The development of new oil fields and improved management techniques has led to a decrease in produced water, whereas the maturation of existing fields has resulted in increased production [1,2]. Figure 1 depicts the separation of fluids in the unit separation process in an oilfield. Worldwide, only one barrel of oil is produced for every four barrels of water. This study focuses on the co-produced water from the Sarir and Jalo oilfields under investigation, as well as the potential use of this water as a renewable energy heat source for electricity production in power plants.

Significant volumes of contaminated water, often known as produced water, co-produced water, or water from oil wells, can be generated during oil production processes. According to Patel [3], produced water is defined as "the water (brine) brought up from the hydrocarbon-bearing strata during the extraction of oil and gas, and can include formation water, injection water, and any chemicals added down hole or during the oil/water separation process."

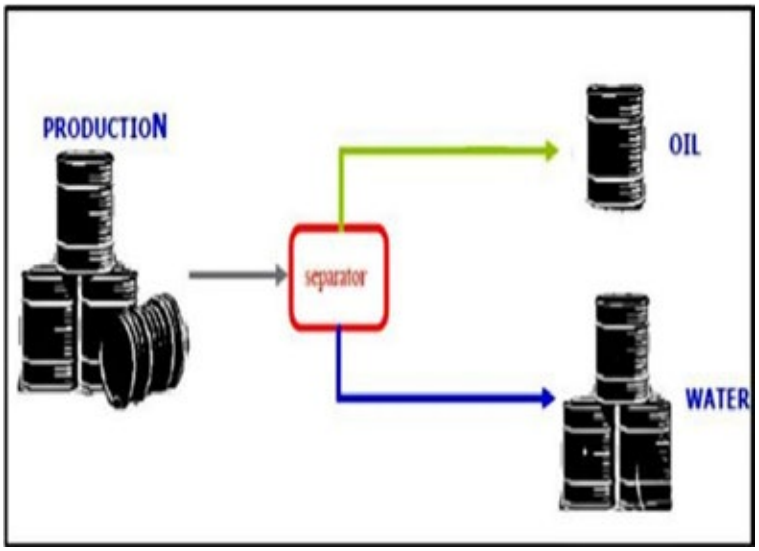

Figure 1. Schematic of a basic separation unit for produced fluids.

Figure 2 shows the production curve for co-produced hydrocarbons and water in a typical oilfield. The graph demonstrates how the W/O ratio changes significantly as an oilfield matures, with water accounting for a large portion of the output [4].

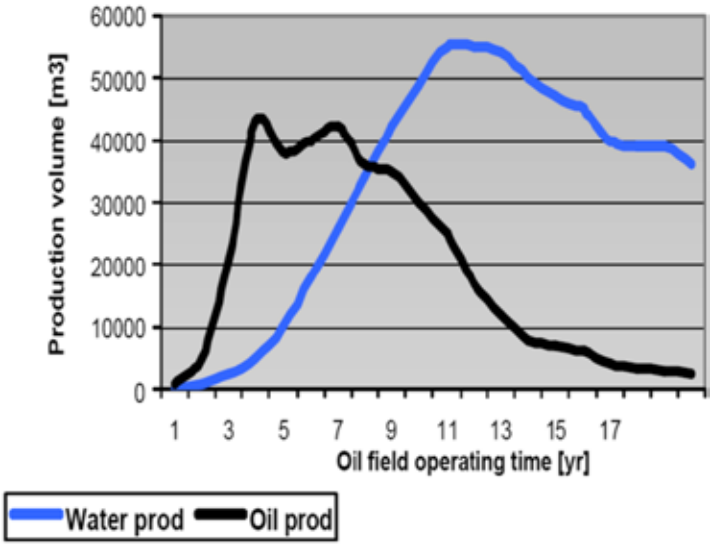

Figure 2. Typical production profile for an oilfield in the North East Atlantic [4].

The applications of co-production from operating hydrocarbon wells and converting abandoned wells to geothermal wells are quite different. The wellhead temperature, fluid flow rate, and water cut (W/C) are the three most critical variables for successful co-production deployment. The electrical power produced by hydrocarbon fields ranges from a few hundred kW to several megawatts (MW) [5].

In this research, the term "co-production" refers to the simultaneous extraction of geothermal energy and hydrocarbons from the same oil well or oil field. This method harnesses heat and/or power from the heat contained in co-produced geothermal fluids of oil and gas operations, often brines [6]. By reducing energy costs, geothermal co-production aims to extend the economic life of a field and/or generate revenue by selling excess energy output back to the grid. This approach ultimately increases the amount of oil and gas recovered, delaying the field's abandonment date and increasing oil and gas sales revenues.

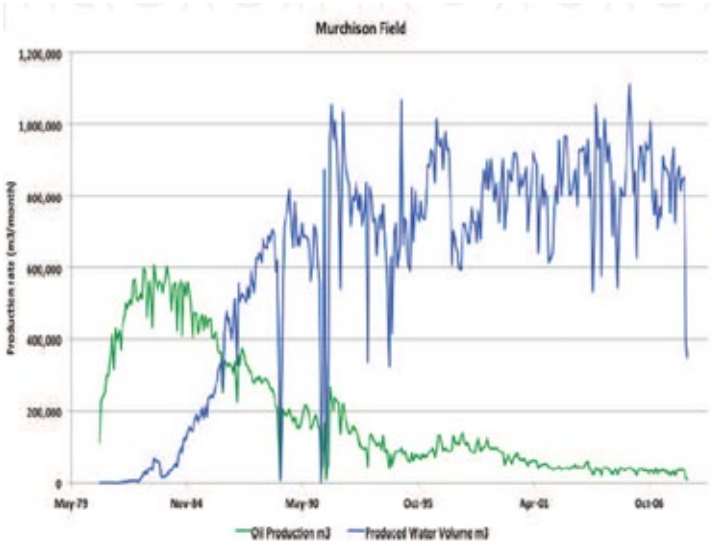

Figure 3. Oil and water production profile for the Murchison field, North Sea [7].

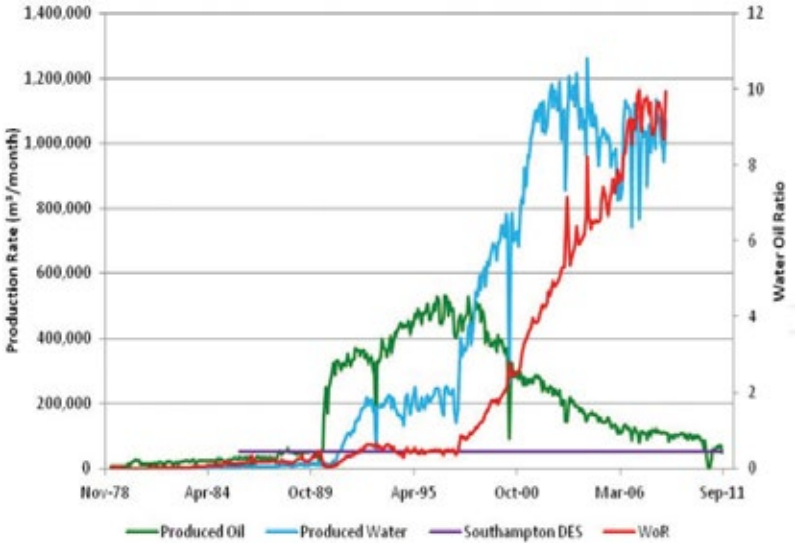

Figure 4. Wytch Farm Field in Dorset is the UK's Jon, et al.[7].

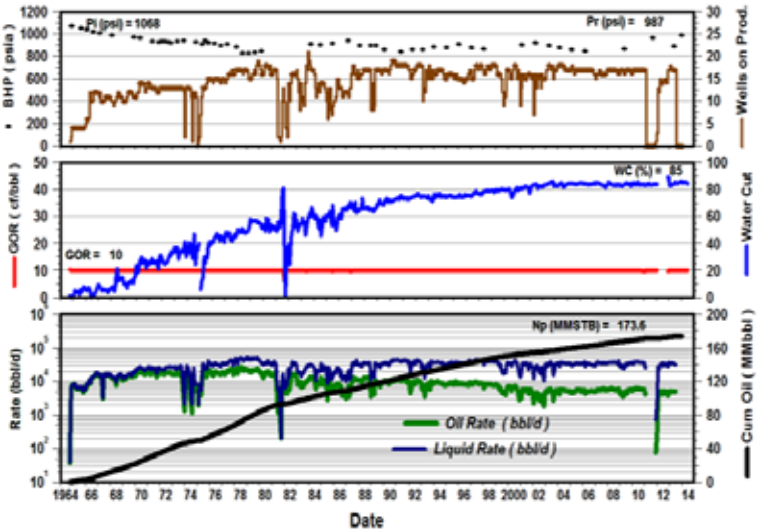

Figure 5. The production performance plots for the Jalo oilfield [8].

Co-production also benefits the environment. The electricity from geothermal sources can offset the use of traditional fuel-burning electricity, thereby reducing the amount of greenhouse gases released during a well's operation by using less fuel [5]. According to Jon, et al. [7], the world produces more than 300 million barrels of water per day, which could provide up to 15,000 MW of power. In certain oil fields, oil production rates have declined, whereas water production rates have increased. Figures 3 through 6 present examples of historical fluid generation in these oil fields.

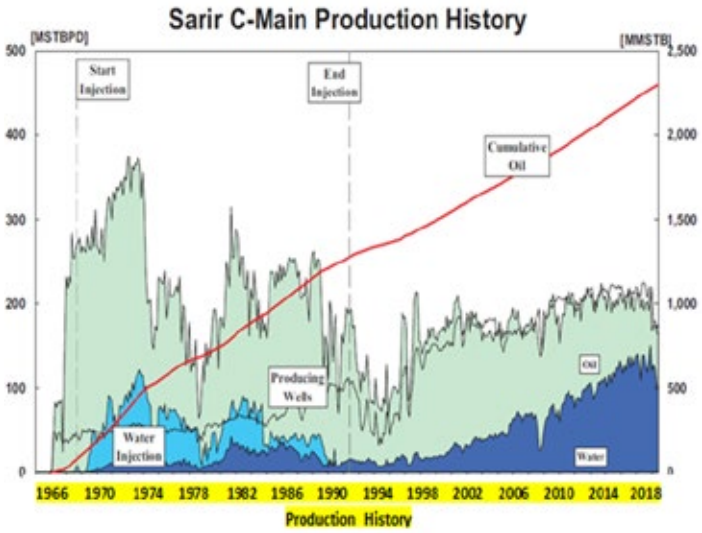

Figure 6. Sarir C-Main production history [8].

This investigation focused on the joint production of several producing wells in the Jalo and Sarir oilfields. Figure 7 shows the locations of the two fields.

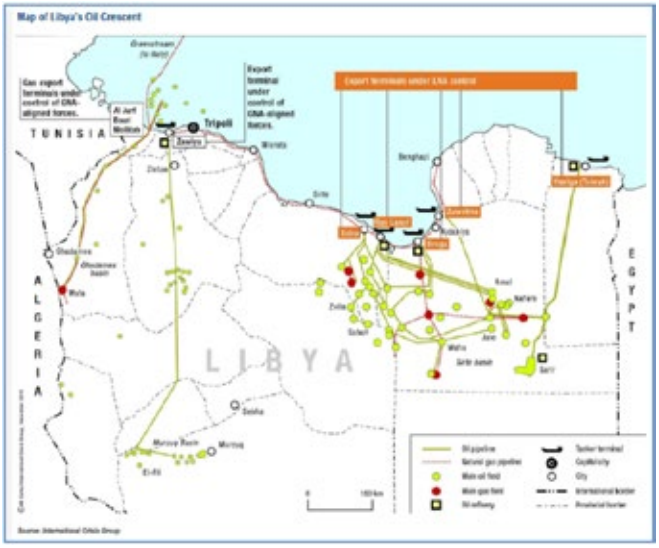

Figure. 7. Map of Libyan's oilfields [8].

The study's significant advantages, which promote the expansion of geothermal power generation, demonstrate its importance for geothermal energy:

1. Geothermal energy is a reliable source of energy.
2. Renewable energy is derived from geothermal sources.
3. The low air emissions from geothermal energy offset the high air emissions from fossil fuel-

burning power plants.
4. Geothermal energy can mitigate other environmental impacts.
5. Geothermal energy does not require combustion.
6. Geothermal energy has a minimal impact on the terrain.
7. Considering environmental costs, geothermal energy competes favorably with other energy methods.
And the main objectives of this study is the potential to utilize oilfield infrastructure to produce geothermal electricity profitably, in a process called co-production. The study also explores the latest advancements in oil and geothermal production and their techniques for co-producing geothermal energy.
The research question for this study is as follows:
1. How much renewable energy can be generated through the sharing of geothermal energy?
2. As the global population increases, so does the demand for energy.
3. Does the generation of electricity via geothermal energy contribute to sustainable development?

2. METHODOLOGY

The study will be based on the World Energy Assessment report (WEA, 2000), United States Department of Energy (US DOE) and the World Energy Council (WEC). The co-produced water data under consideration of the investigated oil wells has been collected and obtained from the internal technical reports of the periodical well testing techniques that running in the oil fields aiming to evaluate reservoirs and well characterizations throughout measuring some important parameters e.g., bottom hole pressure and temperature. The calculations of this data under consideration were performed using the standard mathematical equations and correlations of graphical charts via software programs and Excel approaches. The investigation is founded on a correlation for thermal efficiency obtained from multiple real binary plants. Thermal efficiency, according to conventional definitions, is the ratio of net power production to the heat input rate, or input thermal power. All the plants were subjected to organic Rankine cycles (ORCs). DiPippo [9] is the source of the data used for efficiency. Several studies [10-13] have been conducted on waste heat recovery in oil field applications [14-16]. The Pleasant Bayou field demonstration power plant preceded these studies, where existing wells were used to generate electricity and extract gas and hot water [17]. More recently, a 250 kW Ormat ORC power plant was developed to utilize low-enthalpy energy from co-produced hot water at the Teapot Dome Field, Wyoming, USA. [14] reported that the combination of co-produced gas and water in an abandoned gas well in Texas could generate 340 kW of net electricity. According to [18], geothermal power generation in the Los Angeles Basin oilfields could yield a net power output of approximately 7430 kW. Another assessment of co-produced fluid geothermal power generation using an analytical model based on thermodynamic heat balance combined with mass balance was carried out by [19] in the Wytch Farm oilfield in the United Kingdom.Recent advancements in the geothermal industry have been noted according to [20]. This study addresses direct heat usage and power plant technology advancements. Geothermal utilization has been proposed as a substitute for current fossil fuels to significantly reduce emissions in the coming years. The income of a geothermal project could also be increased through direct heat utilization. In a recent study, [21] examined the feasibility of co-produced fluid geothermal power in the Banks Field within the Williston Basin. The total output in 2018 from the 260 operating wells in the Banks Field was 2.4 million barrels of water and 1.9 million barrels of oil. This study recommended the use of compact, 20–23 kWe ORC power production units. According to [22], several recent studies have been conducted to explore the potential of geothermal energy production. A recent study projected a substantial increase in geothermal utilization by 2050, especially in Europe.
A study conducted in [22] explored the potential for geothermal energy in the Virginia Oil Field.

To assess the potential for power generation over a 25-year period, three different methods were employed. Using a distinct deterministic approach and data from 190 wells, including bottom-hole temperatures and historical water production, the average power potentials of 172 MWt and 28 MWe were determined via the reservoir volume method. They evaluated the average power potential as 115 MWt and 16 MWe. Finally, a total power potential of 199 MWt and 32 MWe was calculated using a Monte Carlo method for heat power.

A study was performed by Robins, et.al., [23] about geothermal energy development in the U.S. primarily focuses on low- and medium-temperature systems, aiming to construct 1-MW geothermal power plants.

According to McClure, et al., [24] geothermal energy offers low greenhouse gas emissions and reliable baseload electricity. Global geothermal capacity currently stands at 11,000 MWe.

Mckittrick [25] presents study about geothermal technologies and utilizing of geothermal power plants for electrical power generation.

According to International Renewable Energy Agency (IRENA) [26, 27] report, the global geothermal capacity in 2023 is mostly dominated by the countries in Asia and North America. Fatick, et al., [28] reported that the U.S. Department of Energy estimates that utilizing just 0.1% of Earth's geothermal resources could meet global energy demands for millennia. Enhanced Geothermal Systems (EGS) have emerged as a promising technology for sustainable energy production, offering significant potential for clean, renewable heat extraction from deep geothermal reservoirs.

3. GEOTHERMAL RESOURCES

Natural aquifers contain hydrothermal resources, which are a type of deep geothermal energy. Enthalpy can be used to categorize these aquifers into high and low enthalpy groups. High enthalpy systems can utilize flash or dry-steam processes, whereas low enthalpy systems require the organic Rankine cycle (ORC) or the Kalina process. As shown in Figure 8, [6] proposed classifying geothermal resources on the basis of their enthalpy, temperature, and pressure. The enthalpy is a characteristic of a thermodynamic system and can be defined as the system's internal energy plus the product of its pressure and volume.

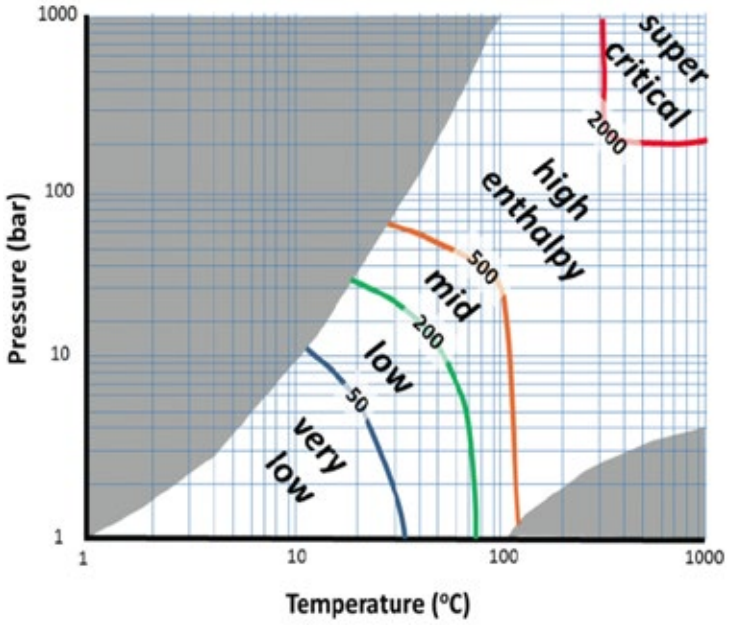

Figure 8. Categorization of geothermal resources. The numbers on the lines represent approximate values of enthalpy in kJ/kg [6].

Geothermal power plants for electrical power generation are now in use in various parts of the world with current technologies [5]. The geothermal power plant is depicted in Figure 9.

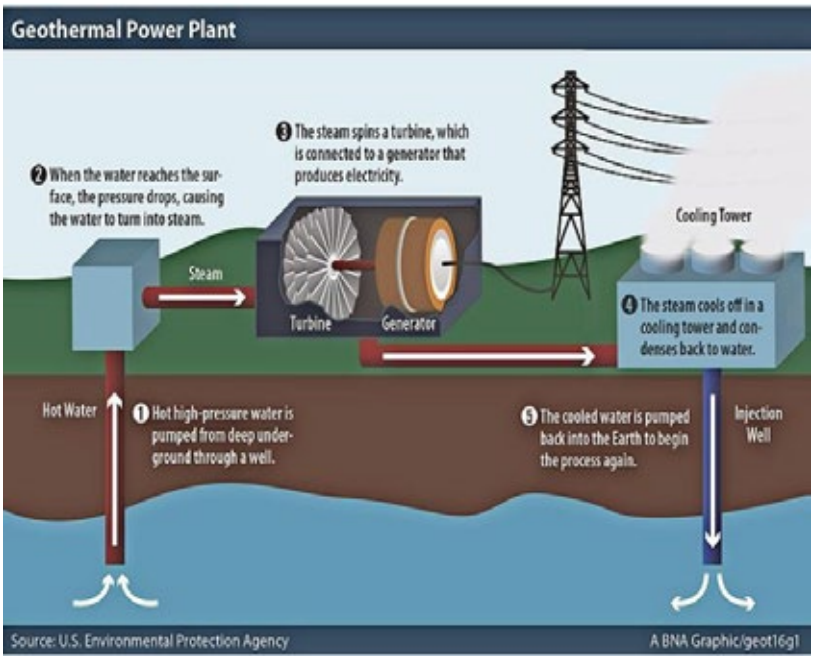

Figure 9 Geothermal electricity power plant [5].

3.1. Electric Power Generation

One of the primary applications of geothermal energy is generating electricity through three main types of geothermal power plants: dry steam, flash steam, and binary (Figure 10). Each power plant layout has different energy conversion efficiencies and operational requirements, impacting the sustainable management of geothermal resources. Proactive management of plants and reservoirs is necessary, as operational features influence reservoir performance.

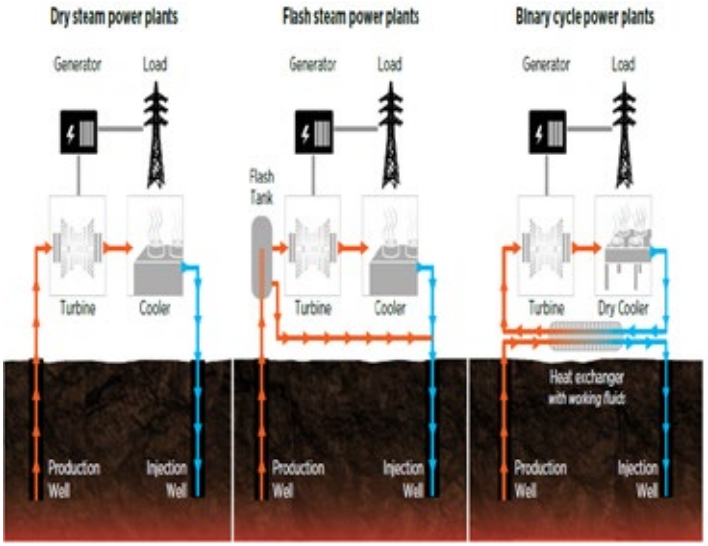

Figure 10. Geothermal power-plant configuration: dry steam, flash steam, and binary cycle [29].

3.2. Electricity from Co-produced Oil Operations

According to recent suggestions, hot fluids produced alongside oil and gas activities may contain significant untapped hydrothermal energy potential [29]. On the basis of the fluids already

produced in seven Gulf Coast states, the authors estimated that the resource potential could range from approximately 985–5,300 MWe (depending on the water temperature). The utilization of geothermal fluids at low to moderate temperatures through binary power plants is a proven method, as described by DiPippo [9], [30]. A simplified representation of a typical binary plant is shown in Figure 11. Energy recovery from coproduced fluids is best suited for this type of operation.

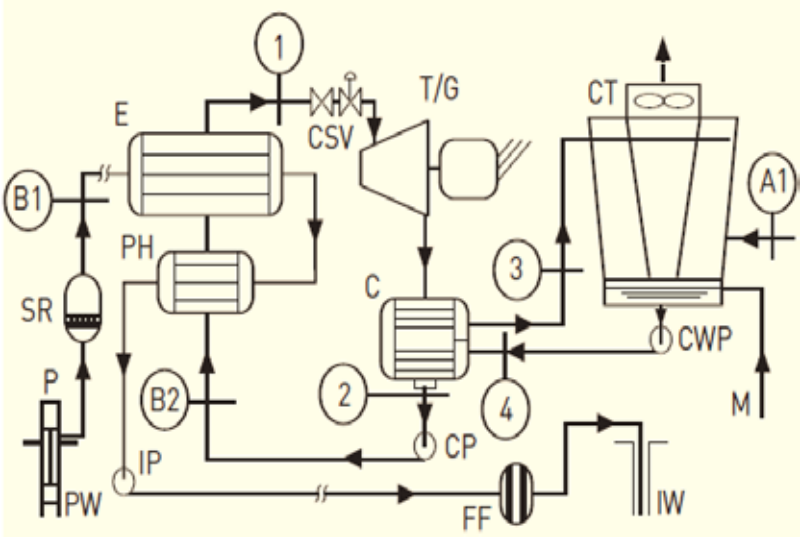

Figure 11. Basic binary power plant in simplified schematic form [30].

3.3. Binary Power Plants

Binary power plants are a well-established method for extracting energy from coproduced fluids in oilfields at low temperatures. In a binary power plant, a secondary working fluid that boils at a lower temperature is heated by the geothermal fluid. The turbine is operated, and energy is generated via the working fluid, not the geothermal fluid itself. Common working fluids include water–ammonia mixtures for the Kalina cycle, hydrocarbons (e.g., pentane and isobutene), and refrigerants (R123, R134a, and R245FA). Whether these fluids are combustible or toxic is irrelevant the working fluid is contained in a closed cycle and does not come into contact with the external environment. Figure 12 shows a simplified schematic of a binary cycle.

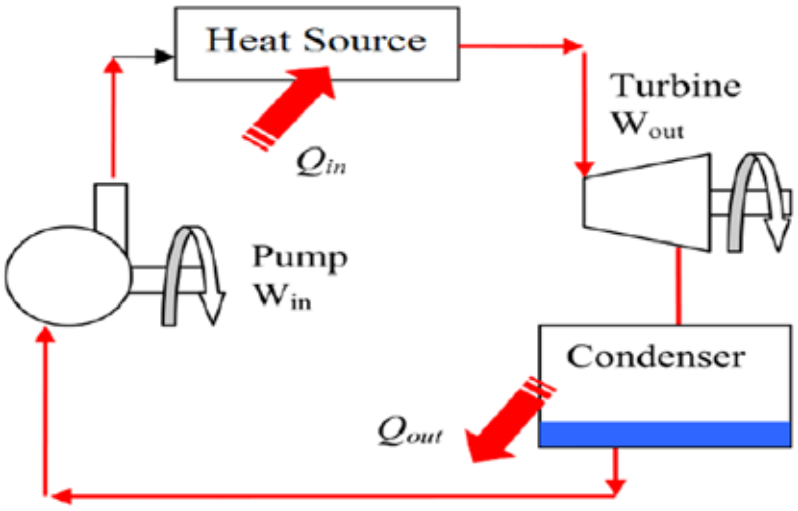

Figure 12. Simplified schematic diagram of the Rankine binary cycle [31].

All four processes in an ideal Rankine cycle are reversible, as illustrated in the temperature vs. specific entropy diagram (T-S) (Figure 13).
1-2: The working fluid begins at state 1 and is isentropically compressed to a higher pressure at state 2 after entering the pump as a saturated liquid.
2-3: A constant pressure is maintained while heating the fluid, which exits the heat source as superheated vapour at state 3.
3–4: The turbine allows the superheated fluid to expand isentropically, generating work, and it exits the turbine as premium vapour at state 4.
4-1: A consistent pressure is used to condense the steam, allowing the fluid to re-enter the pump and return to state 1.

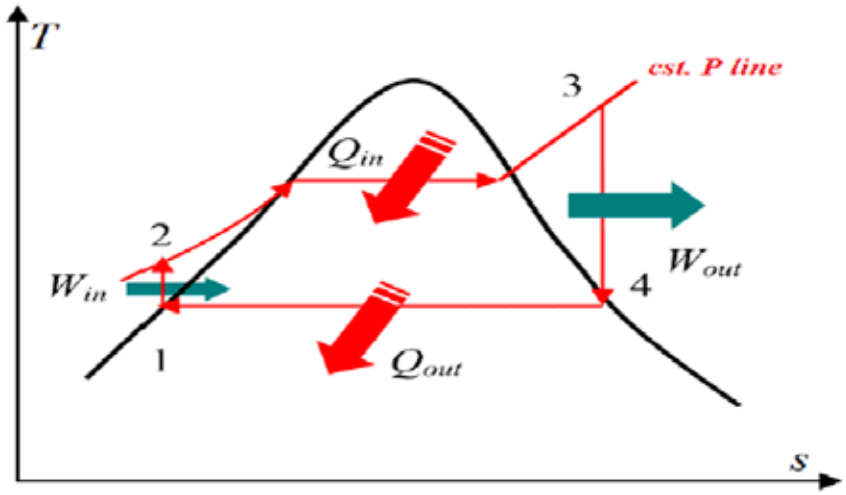

Figure 13. T-S diagram of an ideal Rankine cycle [32].

The first law efficiency, or thermal efficiency, for a perfect Rankine cycle can be expressed via the following equations:

$$\eta_{th} = \frac{W_{net}}{q_{in}} \quad (1)$$

Knowing that:

$$W_{net,in} + q_{in} = W_{turbine,out} + q_{out} \quad (2)$$

We deduce that:

$$W_{net} = W_{turbine,out} - W_{pump,in} = q_{in} - q_{out} \quad (3)$$

and hence:

$$\eta_{th} = \frac{W_{net}}{q_{in}} = 1 - \frac{q_{out}}{q_{in}} \quad (4)$$

The maximum thermal efficiency is constrained by the second law of thermodynamics and can be represented as:

$$\eta_{max} = \frac{T_H - T_L}{T_L}$$

According to Bilbow [33], T_H denotes the temperature at which heat is supplied to the working

fluid, whereas T_L indicates the temperature where heat is released to the condenser from the working fluid.

3.4. Net Thermal Efficiency in Relation to Geofluid T1

Tester [28] examined the influence of the inlet temperature of a geofluid (T1) on the cycle thermal efficiency by evaluating the performance of 10 modern binary power plants. The thermal efficiency of the cycle was determined using the ratio of the net power produced to the heat intake rate, as expressed in Eq. (5):

$$\eta_{th} = \frac{\dot{E}}{\dot{Q}} \qquad (5)$$

The temperatures of the geofluids in the binary power plants surveyed ranged from 103°C to 166°C. For this study, performance data from an additional ten low-temperature binary power plants were considered to establish the relationship between the geofluid temperature and cycle thermal efficiency since the targeted coproduced geofluids in this research were below the range of those in Tester's [28] survey. The correlation for net thermal efficiency as related to geofluid temperature was obtained with 20 power plants in the expanded survey, presented in Eq. (6):

$$\eta_{th} = 0.0927\ T_{in} - 2.068 \qquad (6)$$

where T_{in} represents the temperature in degrees Celsius, and ηth is the percentage of net thermal efficiency.

The correlation provided by Tester [34] can be utilized to calculate the cycle's net thermal efficiency on the basis of the temperature of the coproduced fluid:

$$\eta_{th} = 0.0935\ T_{in} - 2.3266 \qquad (7)$$

where

η_{th} = cycle thermal efficiency (%)

T_{in} = inlet temperature in °C

The analysis presented was based on a correlation for thermal efficiency derived from various actual binary power plants. The conventional understanding of thermal efficiency is defined as the ratio of net power generation to the heat input rate, or input thermal power [23]29.

The working fluid in the Húsavík plant consists of a mixture of water and ammonia, and [9] provides details about the data utilized for efficiency, which were compiled from multiple sources. The net power output can then be calculated via the geofluid input temperature, output temperature, and mass flow rate.

3.5. Specific Power

The net power output of the power plant was determined on the basis of the geofluid mass flow rate, along with the inlet and outlet temperatures of the geofluid, using the correlation equation shown in Eq. (7). The specific power output, as a function of the designated geofluid outlet and inlet temperatures, is depicted in Figure 14 and expressed by Eq. (8):

$$SP = \left(\frac{0.0927\ T_{in} - 2.068}{100} \right) \left[h(T_{in}) - h(T_{out}) \right] \qquad (8)$$

where *SP* represents the specific power in kW/kg/s; T_{in} and Tout are the geofluid temperatures entering and exiting the power plant, respectively, in degrees Celsius; h (T_{in}) indicates the enthalpy of the geofluid at the inlet, in kJ/kg; and h (T_{out}) denotes the enthalpy at the outlet, in kJ/kg.

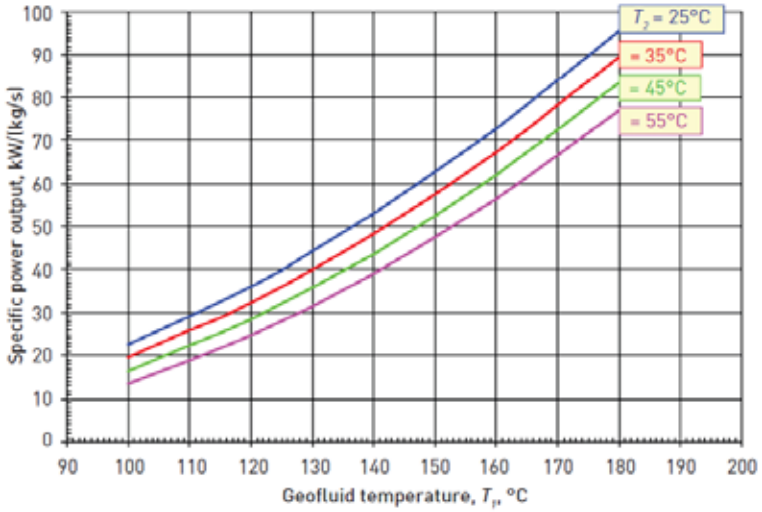

Figure 14. Specific power output (in kW/(kg/s)) for low- to moderate-temperature geofluids as a function of inlet (T_1) and outlet temperatures (T_2) is shown in degrees (°C).

4. RESULTS AND DISCUSSION

The feasibility of the study relies on several key factors, including the temperature of the geothermal fluid, the overall flow rate, and the water cut, which is defined as "the proportion of water produced in relation to the total liquid volume produced" (Schlumberger Glossary). The temperature must meet a minimum threshold to ensure effective vaporization of the working fluid, with higher temperatures being more favorable. The lowest fluid temperature used for electricity production was 74°C [29]. Higher water flow rates, provided the temperature is adequately high, lead to a greater volume of working fluid being vaporized.

4.1. Jalo Oilfield

4.1.1. Co-produced Geothermal Resource Analysis

The document details the findings of Jalo study on generating electricity using co-produced water from five oilfield wells (refer to Table 1). The water's characteristics are as follows:

1. The carbonate formation has a reservoir temperature of 88°C at a depth of 7990.50 feet.
2. The combined flow rate of co-produced hot water from the five wells at the gathering center is 6,658 BWPD.
3. The fluid exiting the ORC plant has a wellhead temperature of 70°C and a rejection temperature of 35°C.
4. The brine entering the ORC power plant has an inlet temperature of approximately 60°C.

Table 1 lists the primary geothermal fountain wells selected in the Jalo oilfield.

Well No.	BFPD (bbl/d)	BOPD (bbl/d)	BWPD (bbl/d)	W/C	Wellhead pressure (psi)	Bottom hole pressure (psi)	Well depth (ft)	GOR (scf/ STB)	Water temperature (°C)
GX1	1470	250	1220	0.83	310	1812	9873	52	220
GX2	1667	277	1390	0.84	230	2730	7900	120	213
GX3	1610	195	1415	0.88	212	2647	8910	129	207
GX4	1560	215	1345	0.86	384	2710	8952	233	190
GX5	1443	155	1288	0.89	242	2675	9157	190	201
Σ	7750	1092	6658						
$\bar{X}$				0.86	275.6	2514.8	8958.4	144.8	206.2

4.1.2. Properties of the Reservoir and Fluid

Table 2 presents a summary of the reservoir and fluid properties for the wells in the Jalo field.

Table 2. Properties of the reservoir and fluid in the Jalo field.

Reservoir characteristics	
Formation (Lithology)	Carbonate
Average depth (ft)	8958.4
Average pay thickness (ft)	42.5
Permeability range (m Darcy)	120-340
Average porosity (%)	17-22
Reservoir temperature (°C)	94
Oil characteristics	
Viscosity (cp)	0.38-1.85
Oil gravity (°API)	36.8
Kinematics viscosity @ 100 °F, cst	12.15
Salt content as NaCl, lb/1000 bbl	4.01
Acidity, mg KOH/g	0.075

4.1.3. Data on Temperature and Production

The temperature and production data can be described as follows:
The combined production rate of the wells is 6658 barrels of water per day (BWPD).
The temperature of the water produced from all five wells, exiting the "knockout" tank at a rate of (6658×159/24×60×60) = 12.25 kg/s was calculated to be approximately 60°C.
The temperature of the co-produced water, post separation, at the inlet of the ORC plant was approximated to be 60°C (=T_H).
The location experiences ambient temperatures ranging from 65 to 115 °F. The water produced at approximately 65°C by the five wells likely provided adequate heat and flow to operate an ORC power plant.

4.1.4. Flow Rates at the Gathering Center (GC1)

The flow rates for the five wells GX1, GX2, GX3, GX4, and GX5 were determined as follows:
QGX1 = 0.83 × 193.99 = 161.01 m3/day
Here, 83% represents the water cut (w/c), and 193.99 (1220/6.289) denotes the volume of produced water in cubic metres (m3). Similar calculations were performed for the other wells, as shown below:

Q_{GX2} = 0.84 × 221.02 = 185.66 m^3/day
Q_{GX3} = 0.88 × 224.99 = 197.99 m^3/day
Q_{GX4} = 0.86 × 213.87 = 183.92 m^3/day
Q_{GX5} = 0.89 × 204.80 = 182.27 m^3/day

The coproduced water flow rates from the five wells after separation are estimated as follows:
The total flow rate is calculated as 161.01 + 185.66 + 197.99 + 183.92 + 182.27, which equals 910.85 m^3/day or 5,728.34 BWPD. These calculated values are listed in Table 3.

Table 3: The calculated coproduced water flow rates.

S/N	Well No.		Flow rate
1	GX1	Q_{GX1}	161.01 m^3/day
2	GX2	Q_{GX2}	185.66 m^3/day
3	GX3	Q_{GX3}	197.99 m^3/day
4	GX4	Q_{GX4}	183.92 m^3/day
5	GX5	Q_{GX5}	182.27 m^3/day
Σ			910.85 m^3/day 5,728.34 BWPD

Table 4: Operation data and different parameters for oil wells in the Jalo field.

S/N	Parameters	Values
1	Cumulative liquid production from 5 wells	7750 (bbl/day)
2	Coproduced water	910.85 (m3/d) 5,728.34 (bbl/d)
3	Ambient temperature	65 to 115°F
4	Average reservoir temperature	94°C (201.2 °F)
5	Inlet water temperature (measured)	60 °C (140 °F)
6	Outlet water temperature (approximated) (Tc)	35 °C (95°F)

With respect to the power output analysis, MIT Tester [34] suggested that the cycle net thermal efficiency can be determined from the temperature of the coproduced fluid via the following correlation equation (7): $\eta_{th}=0.0935\ T_{in}-2.3266$, where η_{th} represents the cycle thermal efficiency (%) and T_{in} represents the inlet temperature in °C. Therefore, when T_{in} is 60°C, the cycle thermal efficiency is calculated as $\eta_{th}=0.0935\ (60)-2.3266$, which equals 3.28%.
However, the calculations of electric power are detailed in Table 5.

Table 5. Electric power calculations.

S/N	Parameters	Values
1	Co-produced water	910.85 (m3/d) 5,728.34 (bbl/d)
2	Inlet water temperature (measured)	60°C (140 °F)
3	Outlet water temperature (approximated) (Tc)	35°C (95°F)
4	BTU per °F per bbl	350
	Available thermal power	
1	Total heat content = (350) (140 – 95) × (5,728.34) = 90,221,355 = 90.2x 10^6 BTUs/day	
2	Thermal power = BTUs/24 hr × 0.00029307107 = 1101.45 kWth	
	Output electric power	
1	Thermal efficiency of ORC cycle = 3.28% (MIT, 2006)	
2	Power generated = 0.0328 × 1101.45 = 36.13 kWe	

In accordance with the Massachusetts Institute of Technology (MIT), Tester [28] introduced a different method for calculating the net electric power output of the ORC power plant. After the cycle net thermal efficiency is determined, the net power output can be calculated via the geofluid (brine) inlet temperature, the geofluid outlet temperature, and the geofluid mass flow rate. The results are presented in Figure 16.

The graph provides the power output (in kW) for a unit mass flow rate of one kg/s on the basis of the inlet (T_1) and outlet (T_2) geofluid temperatures. The total power output can be obtained by multiplying this value by the actual mass flow rate in kg/s. For example, a flow of 20 kg/s of geofluid at 130°C discharged at 35°C can be estimated to yield a power output of 800 kW (i.e., 40 kW/(kg/s) times 20 kg/s). Furthermore, a flow of 30 kg/s of geofluid at 110°C discharged at 25°C can be estimated to yield a power output of 900 kW (i.e., 30 kW/(kg/s) times 30 kg/s).

Using the methodology outlined by MIT, Tester [28], we can estimate the electric power output from co-produced water at five wells in the Sarir field based on the following data:

- The brine temperature at the inlet of the geofluid is 60°C.
- The outlet temperature is 35°C.
- The geofluid mass flow rate is 12.25 kg/s.

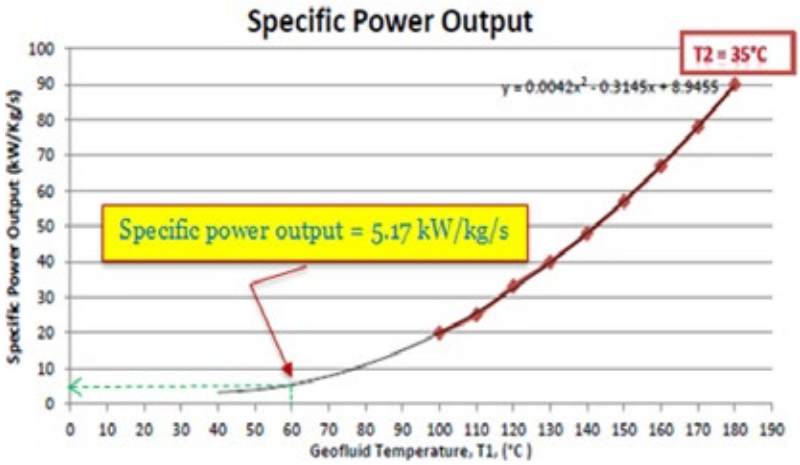

Figure 15. Backwards extrapolated curve of the specific power output for T_2 = 35°C.

To determine the specific power output for the inlet temperature (T_1) of 60°C, the curve was extrapolated backwards from Figure 15, which represents the specific power output for an outlet temperature of 35°C.

According to the extrapolated curve in Figure 15, the specific power output for an inlet temperature of 60°C is calculated as 5.17 kW/kg/s.

The gross electric power output from co-produced water in the Sarir Field is estimated to be 63.33 kW, calculated as 5.17 kW/kg/s multiplied by 12.25 kg/s. The analysis was conducted at a gathering center associated with five producing wells that generate water along with hydrocarbons in the Sarir oilfield, located in the Sirte Basin, Libya.

The study indicates that this gathering center has the potential to produce a gross power output of 63.33 kW at an ORC power plant outlet temperature of 35°C using produced water from five high W/C wells. This technology can be scaled up to include the entire Jalo field, resulting in significantly greater electricity generation and economic viability.

Previous research by Bennett [18] has shown that fields with moderate temperatures but high flow rates are often economically viable, highlighting the importance of sufficient flow rates over reservoir temperature. Even lower production temperatures can be offset by higher production

rates, explaining why the most economically productive fields prioritize sufficient flow rates rather than the highest temperatures.

4.2. Sarir Oilfield

The second gathering center (GC2) also includes five producing wells but with different characteristics from those of GC1, particularly in terms of flow rates and temperatures. These wells are known as SX1, SX2, SX3, SX4, and SX5, as shown in Table 6.

Table 6: Primary Geothermal Wells Selected in the Sarir Oilfield.

Well No.	BFPD (bbl/d)	BOPD (bbl/d)	BWPD (bbl/d)	W/C	Wellhead pressure (psi)	Bottom hole pressure (psi)	Well depth (ft)	GOR (scf/ STB)	Water temperature (°C)
SX1	4130	950	3180	0.77	195	1995	9870	98	220
SX2	5172	1052	4120	0.80	230	2600	9800	110	244
SX3	5947	845	5102	0.86	280	2520	8910	120	232
SX4	4105	1110	2995	0.73	250	2850	8950	205	210
SX5	4197	1089	3108	0.74	244	2702	9152	155	230
Σ	23551	5046	18505						
$\bar{X}$				0.78	239.80	2533.4	9336.4	137.6	227.2

4.2.1. Temperature and Production Data

The temperature and production data for the wells are as follows:
1. The combined production from the wells is 18,505 barrels of water per day (BWPD).
2. The temperature of the combined produced water from these five wells, as it exits the "knockout" tank at 18,505 × 159 / (24 × 60 × 60) = 34.05 kg/s, is estimated to be approximately 70°C.
3. The temperature of the co-produced water at the inlet of the ORC plant, after separation, was determined to be 70°C (TH).
4. The site experiences ambient temperatures ranging from 75 to 100°F. The water produced at approximately 75°C by the five wells likely provides sufficient heat and flow for operating an ORC power plant.

4.2.2. Co-produced Geothermal Analysis

This report presents the findings of the feasibility study on generating electricity using co-produced water from the five wells in the second gathering center (SC2) (Table 6), which exhibit the following characteristics:

1. The temperature of the reservoir formation is 94°C at a depth of 8,920.2 feet.
2. The combined flow rate of co-produced hot water from the five wells in the gathering center is 18,505 BWPD.
3. The fluid rejection temperature exiting the ORC plant was set at 35°C, with a wellhead temperature of 70°C.
4. The inlet temperature of the brine entering the ORC power plant was approximately 70°C.

4.2.3. Well Characterization Parameters

The key parameters for estimating electricity generation from the investigated wells are represented graphically. Two parameters that significantly affect the power generation of co-produced water

are as follows:

1. Co-produced rate (bbl/day, cubic meter/day, kilogram/second, liter/second).
2. Co-produced temperature (°C).

4.2.4. Calculating Flow Rates at the Gathering Center (GC2)

The flow rates of wells SX1, SX2, SX3, SX4, and SX5 were determined as follows:
The flow rate of well SX1, QSX1, was calculated as 0.77 multiplied by 505.65, resulting in 389.35 m^3/day.
Here, 77% represents the water cut (w/c), and 505.65% (3180/6.289) represents the water produced in cubic metres (m^3). Similar calculations were carried out for the other wells:
$Q_{SX2} = 0.80 \times 655.11 = 524.09$ m^3/day
$Q_{SX3} = 0.86 \times 811.26 = 697.68$ m^3/day
$Q_{SX4} = 0.73 \times 476.23 = 347.65$ m^3/day
$Q_{SX5} = 0.74 \times 494.20 = 365.71$ m^3/day
The total flow rate of co-produced water from the five wells after separation is estimated as:
Total flow rate = 389.35 + 524.09 + 697.68 + 347.65 + 365.71 = 2324.48 m^3/day = 14618.65 BWPD
In summary, Table 7 presents the calculated values of the co-produced water flow rates of the investigated producing oil wells.

Table 7. Calculated values of the co-produced water flow rates.

S/N	Well No.		Flow rate
1	SX1	Q_{SX1}	389.35 m3/day
2	SX2	Q_{SX2}	524.09 m3/day
3	SX3	Q_{SX3}	697.68 m3/day
4	SX4	Q_{SX4}	347.65 m3/day
5	SX5	Q_{SX5}	365.71 m3/day
Σ			2324.48 m3/day 14618.65 BWPD

Additionally, Table 8 provides various parameters and operation data for oil wells in the Sarir field.

Table 8. Operation data for oil wells in the Sarir field.

S/N	Parameters	Values
1	Cumulative liquid production from 5 wells	23551 (bbl/day)
2	Coproduced water	2324.48 (m^3/d) 14618.65 (bbl/d)
3	Ambient temperature	65 to 110°F
4	Average reservoir temperature	94°C (201.2 °F)
5	Inlet water temperature (measured)	70 °C (140 °F)
6	Outlet water temperature (approximated) (Tc)	35 °C (95°F)

4.2.5. Analysis of the Power Output

According to Tester [34] at MIT, the cycle net thermal efficiency can be determined from the temperature of the co-produced fluid using the following correlation:

η_{th}=0.0935 T_{in}-2.3266

Where, η_{th} = cycle thermal efficiency (%); and T_{in} = inlet temperature in °C. Therefore, for an inlet temperature of T_{in} = 70°C, the cycle thermal efficiency is calculated as:

η_{th}=0.0935 (70)-2.3266=4.22%

However, the calculations of electric power are presented in Table 9.

Table 9. Electric power calculations.

S/N	Parameters	Values
1	Coproduced water	2324.48 (m^3/d) 14618.65 (bbl/d)
2	Inlet water temperature (measured)	70°C (158 °F)
3	Outlet water temperature (approximated) (Tc)	35°C (95°F)
4	BTU per °F per bbl	350
	Available thermal power	
1	Total heat content = (350) (158 – 95) × (14618.65) = 3.22 x 10^8 BTUs/day	
2	Thermal power = BTUs/24 hr × 0.00029307107 = 3935.25 kWth	
	Output electric power	
1	Thermal efficiency of ORC cycle = 4.22% (MIT, 2006)*	
2	Power generated = 0.0422 × 3935.25 = 166.07 kWe	

* MIT = Massachusetts Institute of Technology (Tester [34])

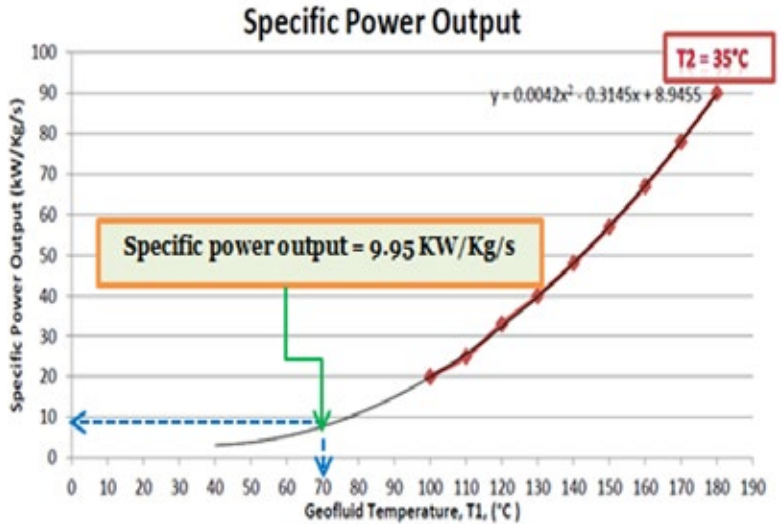

Figure 16. Backwards extrapolated curve of the specific power output for T_2 = 35°C.

The same approach as that of Tester [28] was used at MIT to estimate the electric power output via coproduced water from the five wells at the gathering center in the Sarir field using the following data:

- Inlet geofluid (brine) temperature = 70°C
- Outlet geofluid temperature = 35°C
- Geofluid mass flow rate = 34.05 kg/s

For an outlet temperature of 35°C, we extrapolated the curve backwards, as shown in Figure 16, to determine the specific power output for the geofluid inlet temperature (T1) = 70°C.
The specific power output (for T_1 = 70°C), according to the above curve, can be determined as follows:
Specific power output = 9.85 kW/kg/s.
Hence, the gross electric power output using co-produced water for the Sarir Field can be estimated as follows:
Gross power output = 9.95 × 34.05 = 338.80 kW
This analysis was conducted at the second gathering center (SC2), which involves five producing wells of productive water associated with the producing hydrocarbons for the Sarir oilfield. Overall, this study indicates that this gathering center has the potential to produce a gross power output of 338.80 kW using an ORC power plant outlet temperature of 35°C using produced water from five high W/C wells.

4.3. Comparison of Power Output

Table 10 provides a comparison of the electricity generation outputs for gathering centers GC1 and SC2 in the two case studies. Figure 17 shows the impact of the geofluid mass flow rate and inlet geofluid (brine) temperature (T1) on the gross electric power output for the two cases. It is evident that both the amount of co-produced water flow and the water temperature are correlated with the power output, as depicted in Figure 17.

Table 10. A comparison between the two case studies is presented.

Parameter	Jalo oilfield (GC1)	Sarir oilfield (SC2)
Co-produced water	910.85 (m^3/d) 5,728.34 (bbl/d)	2324.48 (m^3/d) 14618.65 (bbl/d)
Inlet geofluid(brine)temperature (T_1)	60°C	70°C
Outlet geofluid temperature (T_2)	35°C	35°C
Geofluid mass flowrate	12.25 kg/s	34.05 kg/s
Thermal efficiency of ORC cycle	3.28%	4.22 %
Specific power output	5.17 kW/kg/s	9.85 kW/kg/s
Gross electric power output	63.33 KW	338.80 KW

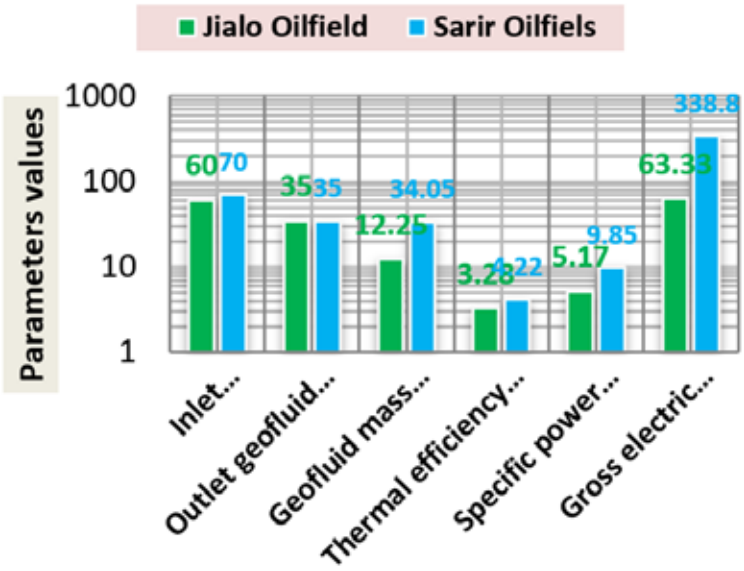

Figure 17 compares the gathering centers GC1 and GC2 for both oilfields.

5. CONCLUSIONS

On the basis of the obtained results, the following conclusions can be drawn:
1. Co-production systems have proven to be cost-effective in various case studies and pilot tests.
2. The key factors for the success of any project are the high temperatures of the produced fluids and, more significantly, a high water flow rate.
3. The use of abandoned wells is particularly appealing for companies in the geothermal sector.
4. Abandoned wells are unable to utilize electricity on site because of the cessation of oil production.
5. Selling the generated energy back to the grid is the sole available option. Consequently, proximity to potential end users and the presence of existing electric infrastructure are crucial factors in selecting wells for energy production.

Author Contributions: All authors have made a substantial, direct, and intellectual contribution to the work and approved it for publication.
Funding: There is no funding for the article.
Data Availability: The data are available at request.
Conflicts of Interest: The authors declare that they have no conflict of interest.

REFERENCES

[1] Dal Ferro, B. and Smith, M. (2007) Global Onshore and Offshore Water Production, http://www.touchoilandgas.com/global-onshore-offshore-water-a7137-1.html,.

[2] Khatib, Z. and Verbeek, P., (2003) "Water to Value – Produced Water Management for Sustainable Field Development of Mature and Green Fields," Journal of Petroleum Technology, 26-28.

[3] Patel, Chirag V. (2004) "Effective Management of Produced Water," MS thesis, Department of Petroleum Engineering, Texas A&M University, College Station.

[4] Clark, C. E. and Veil, J. A., (2009) "Produced water volumes and management practices in the United States. http ://www.ipd.anl.gov/anlpubs/2009/07/64622pdf

[5] Think Geoenergy, (2018) Five Geothermal Projects Under Renewable Funding Program, Netherland. Retrieved July 3, 2018, from: http://www.thinkgeoenergy.com/five-geothermal-projects-under-renewable-energy-funding-program-netherlands/

[6] Younger, P.L. (2015). Geothermal Energy: Delivering on the Global Potential. Basel:MDPI AG.

[7] Jon G., Alison A., Charlotte A., Catherine Hi., Simon H. and Jonathan C. (2019) Geothermal Potential of the Global Oil Industry. in Renewable geothermal energy explorations. , pp1-1.

https://doi.org/10.5772/intechopen.81062

[8] Arabian Gulf Oil Company (AGCO), (2019) Sarir Field Data base and History File.

[9] DiPippo, R. (2004) "Second Law Assessment of Binary Plants for Power Generation from Low Temperature Geothermal Fluids," Geothermics, V. 33, pp. 565586.

[10] Zhang, L., Yuan, J., Liang, H., Li, K. (2008) Energy from Abandoned Oil and Gas Reservoirs, Proceedings, Asia Pacific Oil and Gas Conference and Exhibition, Perth, Australia.

[11] Davis, A.P., and Michaelides, E.E. (2009) Geothermal power production from abandoned oil wells, Energy, 34.

[12] Bu, X., Ma, W., Li, H. (2012) Geothermal energy production utilizing abandoned oil and gas wells, Renewable Energy, 41.

[13] Barbacki, A.P. (2000) The use of abandoned oil and gas wells in Poland for recovering geothermal heat, Proceedings, World Geothermal Congress, Kyushu – Tohoku, Japan.

[14] Sanyal, S., Bulter, S. (2010) Geothermal Power Capacity for Petroleum Wells-Some Case Histories of Assessment, Proceedings, World Geothermal Congress, Bali, Indonesia.

[15] Xin, S., Liang, H., Hu, B., & Li, K. (2012). Electrical Power Generation from Low Temperature Co-produced Geothermal Resources at Huabei Oilfield. Thrity-Seventh Workshop on Geothermal Reservoir Engineering Stanford University. Stanford.

[16] Cheng, W.L., Li, T.T., Nian, Y.L., Wang, C.L. (2013) Studies on geothermal power generation using abandoned oilwells, Energy 59.

[17] Riney, T.D. (1991) Pleasant Bayou Geopressurised Geothermal Reservoir Analysis, Centre for Energy Studies, University of Texas, Austin.

[18] Bennett, K, Li, K and Horne, R.: (2012) "Power Generation Potential from Coproduced Fluids in the Los Angeles Basin," Proceedings of Thirty-Seventh Workshop on Geothermal Reservoir Engineering Stanford University, Stanford, California, February 1-3.

[19] Singh, H.; Falcone, G.; Volle, A.; Guillon, L. (2017) Harnessing Geothermal Energy from Mature Onshore Oil Fields-The Wytch Farm Case Study. Work. Geotherm. Reserv. Eng., 17,

https://eprints.gla.ac.uk/172301/.

[20] Moya, D., Aldas, C., Kaparaju, P., (2018) Geothermal energy: power plant technology and direct heat applications. s.l. Renew. Sustain. Energy Rev. 94, 1364e0321.

[21] Vraa, H.; Picklo, M.; Hertz, E.; Gosnold, W. (2019) Geothermal Energy Utilization of Multi-Well Oil Pads via the Application Of Organic Rankine Cycle Systems. Trans. - Geotherm. Resour. Counc.., 43, 1078– 1084

[22] Banks, J.; Willems, C. J.; Cowper, A.; Nadkarni, K.; Poulette, S.; Van Allen, C. (2021) Geothermal Power Potential of the Virginia Hills Oil Field, Part of the Swan Hills Carbonate Complex. Proceedings World Geothermal Congress, Alberta, Canada; https://pangea.stanford.edu/ERE/db/WGC/papers/WGC/2020/16050.pdf?t=1590520758.

[23] Robins, J.C., Kolker, A., Flores-Espino, F., Pettitt, W., Schmidt, B., Beckers, K., others, Anderson, B., (2021) US Geothermal Power Production and District Heating Market Report. NREL. No. NREL/TP-5700-78291).

[24] McClure, M., Kang, C., Fowler, G., (2022) Optimization and design of next-generation geothermal systems created by multistage hydraulic fracturing. In: SPE Hydraulic Fracturing Technology Conference and Exhibition. https://doi.org/10.2118/209186-MS. D011S001R006.

[25] Mckittrick, A., (2023) Geothermal technologies office-FY23 mid-year update. https ://www.energy.gov/sites/default/files/2023-03/20230302_McKittrick_AASGMtgatDOE.pdf.

[26] U.S. EIA, (2023) Monthly energy review. Monthly Energy Review, 0035(Junli) 1–278. www.eia.gov/mer.

[27] IRENA, (2024) Renewable capacity statistics 2024. International Renewable Energy Agency, Abu Dhabi. www.irena.org.

[28] Fatick Nath , Md Nahin Mahmood , Ebenezer Ofosu , Aaditya Khanal ; (2024) "Enhanced geothermal systems: A critical review of recent advancements and future potential for clean energy production" ; journal of Geoenergy Science and Engineering, Elsevier, Volume 243, December 2024, 213370.

[29] McKenna, J.R. and D.D. Blackwell (2005) "Geothermal Electric Power from Texas Hydrocarbon

Fields," GRC BULLETIN, May/June, pp. 121128.

[30] DiPippo, R. (2005) Geothermal Power Plants : Principles, Applications and Case Studies, Elsevier Advanced Technology, Oxford, England.

[31] Hettiarachchi, H. M., Golubovic, M., Worek, W. M., & Ikegami, Y. (2007). Optimum design critera for an Organic Rankine cycle using low-temperature geothermal heat sources. Energy, 1698-1706.

[32] Bahrami, M.(2018) -SFU-Canada: http://www.sfu.ca/~mbahrami/ENSC%20461/Notes/Vapor%20Power%20Cycles.pdf

[33] Bilbow, W. M., Brasz, L.J. (2004) Ranking of Working Fluids for Organic Rankine Cycle Applications" (2004) International Refrigeration and Air Conditioning Conference. Paper 722.

[34] Tester, J., Petty, S., Garnish, J., Batchelor, A., Drake, L., Veatch, R., et al. (2006). The Future of Geothermal Energy: Impact of Enhanced Geothermal Systems (EGS) on the United States in the 21st Century. Cambridge: Massachusetts Institute of Technology (MIT).

http://web.mit.edu/newsoffice/2007/geothermal.html.

[35] Holmdann G. (2007). The Chena Hot Springs 400 kW Geothermal Power Plant : Experience Gained During The First Year of Operation. Geothermal Resources Council Transactions 31 : 515- 519.

Table of Nomenclature, abbreviations, symbols and units.

Symbol	Definition	Symbol	Definition
B	Boiler	kW	Kilo watt
BCV	Ball check valve	kWe	Kilo watt electric
bbl	Barrel	lb	Pound
bbl/ d(day)	Barrel per day	LPP	Low pressure pump
BFPD	Barrel fluid per day	LPT	Low pressure turbine
BOPD	Barrel oil per day	M	Make-up water
BWPD	Barrel water per day	m3/d (day)	Cubic meter/day
BTU	British thermal unit	mD	Millidarcy
C	Condenser; compressor, celsius	MR	Moisture remover
CC	Combustion chamber	ORC	Organic Rankine cycle
CP	Condensate pump	P	Pump
CS	Cyclone separator	PH	Preheater
cst	Centistoke	ppm	Part per million
CSV	Control and stop valves	psi	Pound per square inch
CT	Cooling tower	S	Silencer
CW	Cooling water	SAL	Salinity
CWP	Cooling water pump	scf	Standard cubic feet
E	Evaporator	SE/C	Steam ejector/condenser
EC	Economizer	SH	Superheater
F	Flash vessel	SP	Steam piping
FF	Final filter	SPT	Super-pressure turbine
ft	Feet	SR	Sand removal

Symbol	Definition	Symbol	Definition
G	Generator	STB	Stock tank barrel
GOR	Gas oil ratio	T	Turbine
HPP	High pressure pump	T/G	Turbine/generator
HPT	High pressure turbine	TV	Throttle valve
HRSG	Heat recovery steam generator	W/C	Water cut
IP	Injection pump	WP	Water piping
IW	Injection well	WP	Water produced
kg/s	Kilogram/second	WV	Well head valve
η	Efficiency	W	Watt